JOURNAL OF CATALYSIS 96, 408–419 (1985)

The Oxidation Effect on the CO/H_2 Reaction over Titania-Supported Fe Catalysts

L. M. TAU[1] AND C. O. BENNETT

Department of Chemical Engineering, The University of Connecticut, Storrs, Connecticut 06268

Received March 25, 1985; revised June 28, 1985

The activity at 558 K for the CO/H_2 reaction over 10% Fe/TiO_2 catalysts is lower after reduction at 773 K than after reduction at 558 K. Subsequent oxidation of the high-temperature reduced catalyst restores its activity to that which existed after low-temperature reduction. We consider three catalysts: one reduced at 773 K oxidized at 673 K, and then reduced at 558 K (ROXR); one oxidized at 673 K then reduced at 558 K (OXRD); and one simply reduced at 558 K (RDOY). The turnover rates for the CO/H_2 reaction at 558 K are about 100 h^{-1} for each of these catalysts. The bulk compositions measured by Mössbauer effect spectroscopy (MES) are similar for the three catalysts before use. However, the rates of carburization measured by MES are lower for the two oxidized catalysts than for the RDOY catalyst. Also, the surface carbon accumulated on the two catalyst. We propose that the residual difference among these catalysts can be explained by the presence of subsurface oxygen.

INTRODUCTION

The CO/H_2 reaction over supported iron catalysts has been studied in this laboratory over the past few years. Reaction intermediates and reaction sequences have been proposed for the Fe/Al_2O_3 system (*1, 2*). Similar chemical reaction properties were found for Fe/Al_2O_3 and Fe/SiO_2 catalysts during this reaction (*2, 3*). The behavior of Fe/TiO_2 catalyst reduced at various temperatures has been investigated (*4*). For the Fe/TiO_2 system, the CO/H_2 reactivity of the 558 K reduced sample is higher than that of the 773 K reduced sample. In addition, a normal hydrogen chemisorption capacity was found in this system, regardless of the reduction temperature. This is quite different from the other Group VIII metals supported on TiO_2. Possible reasons for this different behavior have been discussed (*4*).

The so-called strong metal–support interaction (SMSI) was first observed by Tauster *et al.* (*5*), and it has been widely investigated since then. By those studies, the effect of the high-temperature reduction (HTRD) of Group VIII metals supported on TiO_2 is generally accepted as caused by a combination of geometric and electronic effects (*4, 6–8, 35, 36*). Tauster *et al.* (*5*) also pointed out that oxidation of the 773 K reduced sample at 673 K followed by reduction at 473 K can completely remove the SMSI effect.

In contrast to the high-temperature reduction effect only a few studies have been made on this high-temperature oxidation effect. Meriaudeau *et al.* (*9*) studied the hydrogenation, dehydrogenation, and hydrogenolysis reactions over TiO_2-supported Pt, Ir, and Rh catalysts. They found that the reactivity of the 773 K reduced catalysts can be totally or partially restored by oxidation of these catalysts at 673 K followed by 473 K reduction in H_2. They explained this oxidation effect in terms of the return of the TiO_2 to its original state. For the Fe/TiO_2 system, Santos and Dumesic (*10*) found that the CO adsorption increases by an order of magnitude when the sample which has been reduced at 798 K is exposed to air at room temperature and then reduced at

[1] Kentucky Center for Energy Research Laboratory, P.O. Box 13015, Lexington, Ky. 40512.

0021-9517/85 $3.00

673 K. In addition, they observed that the Mössbauer spectrum of the paramagnetic component decreased when the HTRD catalyst is exposed to air at room temperature followed by reduction at 693 K (*11*). They concluded that the SMSI can be at least partially destroyed by exposure of the catalyst to air at room temperature. In a previous paper (*4*), we also pointed out that CO/H_2 reaction activity of the 773 K reduced Fe/TiO_2 catalyst increased 50% after exposure of the catalyst to air for 24 h. However, the high-temperature oxidation effect for the Fe/TiO_2 system has never been reported.

We present here a study of the high-temperature oxidation effect on the CO hydrogenation reaction over Fe supported on TiO_2. One sample was reduced at 773 K followed by oxidation at 673 K and then reduced at 558 K. In order to investigate the effect of the high-temperature oxidation on the SMSI, results for the 558 and 773 K reduced catalysts are also presented. The latter is believed to be associated with the so-called SMSI effect and the former is not. In addition, a first oxidized then reduced catalyst was studied to compare the oxidation effect with and without the initial high-temperature reduction. In this work, we used the transient method to study the surface species and reaction sequences. Mössbauer effect spectroscopy (MES) was employed to monitor the catalyst bulk phase during various treatments. The particle size was measured by X-ray diffractometry and compared with the size calculated by hydrogen chemisorption.

EXPERIMENTAL

Catalyst Preparation

The catalyst used in this work is the same as that of the previous study (*4*). Three sample were studied. The common pretreatment of these samples consisted of heating in flowing He at 400 K for 2 h. After this pretreatment one sample was reduced at 558 K for 25 h, we will refer to it as the reduced-only sample (RDOY). Another sample was reduced at 773 K for 16 h then oxidized in pure O_2 at 673 K for 2 h followed by reduction at 558 K for 25 h, this will be the reduced-oxidized-reduced sample (ROXR). Still another sample was oxidized at 673 K in pure O_2 for 2 h followed by reduction at 558 K for 25 h, this will be the oxidized-reduced sample (OXRD). The samples which have just merged from the final reduction processes are called unused samples. During the course of changing temperature in these procedures, the sample was exposed to helium. The gases used in this study were of high-purity grade.

Chemisorption Measurement

The H_2 chemisorption was measured by the so-called flow desorption method (*4*). Hydrogen chemisorption has traditionally been performed in the static mode: however, flow chemisorption techniques have recently been gaining acceptance. Thorough studies have been reported by Freel (*12*) and Sashital *et al.* (*13*). The difference between the traditional static mode and the flow technique has been discussed by Amelse *et al.* (*14*). The advantage of the desorption method, especially for a slow chemisorption process, was discussed by Dalla Betta (*15*). A good agreement of the particle size calculated by this method and other physical means (XRD and TEM) were reported by several authors for supported iron catalysts (*2, 14, 16*). The details of this method have been given by Amelse *et al.* (*14*) and Tau and Bennett (*4*).

Kinetic Measurements and Mössbauer Spectroscopy

The kinetic studies were conducted at atmospheric pressure in a small stainless-steel reactor. The conversions were kept at less than 5% so that the reactor operated in a differential mode. The size range of catalysts particles for the kinetic studies was 590–840 μm. Mössbauer effect spectroscopy was performed in an *in situ* cell. The instrument, flow diagram, and the operating

conditions have been reported elsewhere (*1–4*). Without special mention, all the kinetic experiments were carried out at 558 K and atmospheric pressure. The Mössbauer spectrum was measured at 300 K after quenching from 558 K in CO/H_2.

X-Ray Diffraction (XRD)

X-Ray line broadening experiments were conducted with a Diano-XRD 8000 diffractometer using Cu$K\alpha$ radiation passed through a diffraction monochromater. The experiments were the same as those in a previous paper (*4*).

RESULTS

Chemisorption and XRD Results

Chemisorption results for H_2 are presented in Table 1. It can be seen that after oxidation at 673 K then reduction at 558 K, the H_2 chemisorption capacity of the original 773 K reduced catalyst increased. This result is consistent with previous studies (*5, 9*). The H_2 chemisorption capacities of these samples are ordered OXRD > ROXR > RDOY > HTRD. The particle size measured by X-ray diffraction are also presented in the same table. A good agreement of the particle size calculated by both methods can be found in the table. In general, the XRD and chemisorption results show a similar trend in diameter of particles. However, this is not true for most of the Group VIII metals supported on TiO_2 after reduction at high temperature. Tauster *et al.* (*5*), Baker *et al.* (*17, 18*), Resasco and Haller (*19*), and some other authors found that the particle size is constant regardless of the reduction temperature. However, the chemisorption capacity for the high-temperature reduced catalyst is suppressed. In the Fe/TiO_2 system, a good agreement has been observed by Jiang *et al.* (*16*) and Tau and Bennett (*4*). This result may be caused if (1) the suppression of H_2 chemisorption on Fe/TiO_2 during the SMSI situation is not as strong as other systems; (2) the chemisorption measured for the Fe/TiO_2 system is carried out by the so-called desorption method by both authors. It is worthwhile to point out that the nonsuppression of the H_2 chemisorption does not imply that there is no SMSI effect in the Fe/TiO_2 system (*4*). In addition, although there are differences among the ROXR, OXRD, and RDOY catalysts for the H_2 chemisorption, these differences are quite small.

TABLE 1

Particle Size Characterization and Chemisorption Results for Unused Catalysts

Sample	Chemisorption of H_2 (μmol/g)	Particle size[a] (Å)	XRD result (Å)
ROXR	25.2	288	300
OXRD	31.2	230	280
RDOY	19.6	355	330
HTRD[b]	12.0	600	450

[a] From H_2 chemisorption.
[b] 773 K reduced catalyst.

TABLE 2

Bulk-Phase Compositions of Unused Catalysts after Reduction at Various Conditions

Sample	Fe(0) (%)	Fe^{2+} (%)	$Fe^{8/3+}$ (%)
ROXR	52.8	28.4	18.7
OXRD	50.9	28.9	20.2
RDOY	55.9	29.9	14.2

MES Results on Unused Catalysts

It is interesting to know whether the bulk-phase compositions of these three samples are similar. Mössbauer spectra of these three unused catalysts are presented in Figs. 1a, b, and c. The bulk-phase compositions are shown in Table 2. It can be seen that the RDOY catalyst has the highest quantity of Fe(0) and the OXRD catalyst contains the lowest quantity of Fe(0). This result indicates that the high-temperature oxidation slightly inhibits the subsequent reduction process. In order to illus-

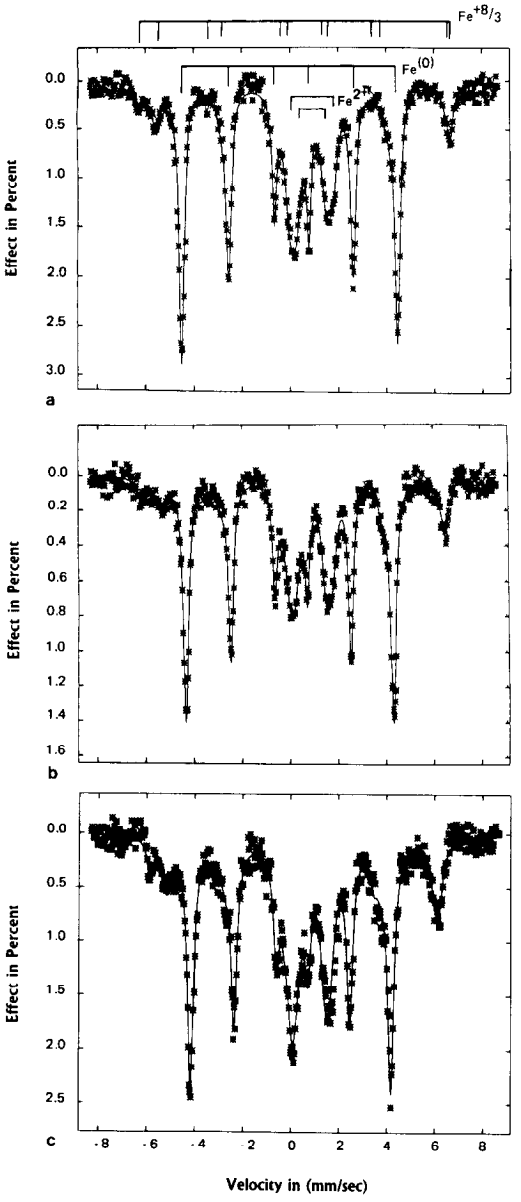

FIG. 1. Mössbauer spectra of unused 10% Fe/TiO_2. Samples: (a) RDOY, (b) ROXR, (c) OXRD.

trate this matter further, another set of Mössbauer results is presented. Figure 2a shows the oven-dried sample, which is the precursor of the RDOY catalyst. Figure 2b shows the sample reduced at 773 K then oxidized at 673 K, which is the precursor of the ROXR catalyst. Figure 2c shows the sample oven-dried and then oxidized at 673 K, which is the precursor of the OXRD catalyst. The bulk-phase compositions of these precursors are listed in Table 3. It can be seen that the α-Fe_2O_3 contents in these samples are ordered Fig. 2c > Fig. 2b > Fig. 2a. From the structural point of view and from the thermodynamic point of view (*20*), α-Fe_2O_3 is more stable than $Fe(NO_3)_3$. In addition, Aharoni (*21*) studied the reduction of iron oxide and proposed that the re-

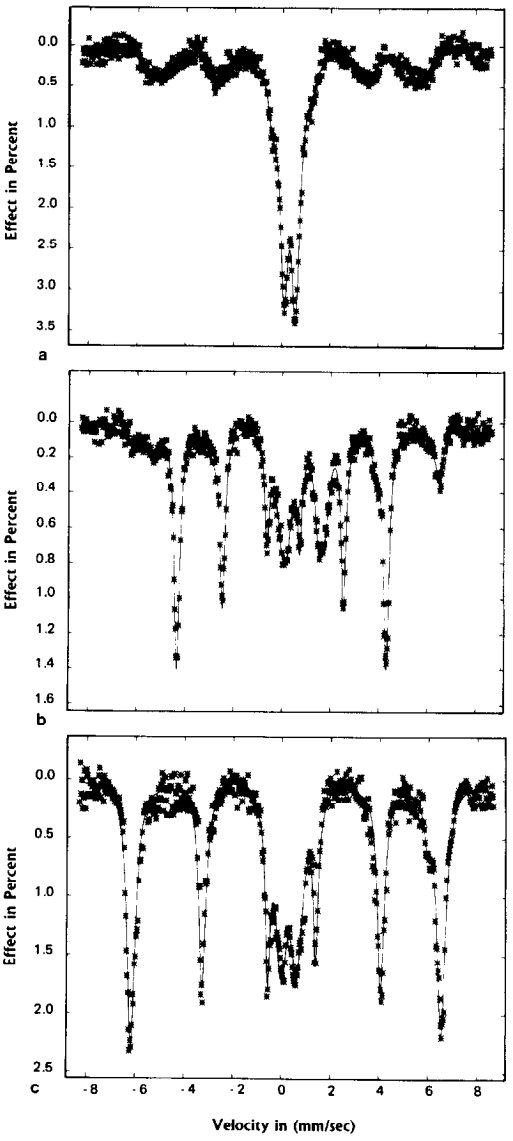

FIG. 2. Mössbauer spectra of catalyst precursors of 10% Fe/TiO_2. (a) Oven-dried only; (b) reduced at 773 K for 16 h followed by oxidation at 673 K for 2 h; (c) oxidized at 673 K for 2 h.

duction process of α-Fe_2O_3 would be

$$\alpha\text{-}Fe_2O_3 \rightarrow \gamma\text{-}Fe_2O_3 \rightarrow Fe_3O_4 \rightarrow FeO \rightarrow Fe(0)$$

Boudart *et al.* (*22*) studied the Fe/MgO system and found that when the small iron particles are oxidized by O_2 at 500 K it converted to γ-Fe_2O_3. Further treatment at 620 K in O_2 transformed the larger particle size to α-Fe_2O_3. This indicates that the α-Fe_2O_3 is stabler than γ-Fe_2O_3.

Following these arguments, it is understandable that the precursor of the RDOY catalyst is the easiest one to reduce among these three samples. This result also indicates that oxidation at any stage, before or after reduction, leads to a difficult reduction. However, in any event, the differences in the bulk-phase compositions among these unused catalysts are small. The hydrogen chemisorption and Mössbauer results of the unused samples show that the physical properties of these three materials are similar.

Kinetic Results

CO/H_2 reaction over unused catalyst. Figure 3 shows the CH_4 formation at 558 K for the four samples. The reactant is 10% CO/H_2. The amount of catalyst is 50 mg and the flow rate is 30 ml/min. It can be seen from the figure that the OXRD catalyst has the highest CH_4 activity per gram of supported catalyst followed by the ROXR and then by the RDOY catalysts. Also shown is the HTRD catalyst, which has markedly reduced activity. It is clear that the activity of the HTRD catalyst has been increased by the oxidation sequences

TABLE 3

Bulk-Phase Compositions of Catalyst Precursors

Sample	ROXR	OXRD	RDOY
α-Fe_2O_3 %	68.27	74.5	—
γ-Fe_2O_3 %	—	—	30.9
Fe + 3%	31.73	25.5	69.1

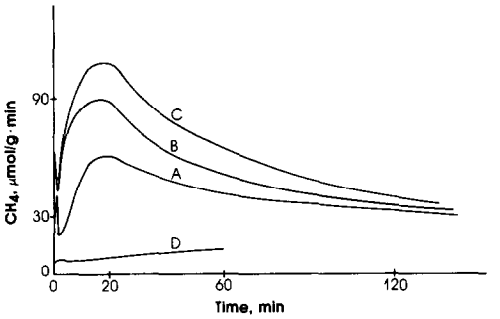

FIG. 3. Rate of CH_4 formation for the reaction of 10% CO/H_2 at 558 K over 10% Fe/TiO_2 treated under various conditions. Samples: (A) RDOY, (B) ROXR, (C) OXRD, (D) HTRD (773 K).

(ROXR) so that its activity is even higher than the RDOY catalyst (LTR catalyst, (*4*)). The highest activity is obtained by avoiding any HTRD, the case for the OXRD sample.

Assuming one site per H atom, the turnover rates for CH_4 formation after 20 min can be calculated from Fig. 3 and Table 1. The results are: OXRD, 102 h^{-1}; ROXR, 106 h^{-1}; RDOY, 95 h^{-1}; and HTRD, 22.5 h^{-1}. Thus, all the catalysts with a final low-temperature reduction are similar; the HTRD catalyst is in a separate category. Supposedly, the low activity of the HTRD catalyst arises from a SMSI effect and not from a supposed particle size effect, such as that observed for Fe/MgO catalysts (*22*), associated with structure sensitivity.

We repeated the kinetic studies using 33% CO/H_2 and 6.5% CO/H_2 instead of using 10% CO/H_2. The same trend has been observed in these reactions and the results are presented in Fig. 4. These results confirmed that the preoxidation of the catalyst gives a higher CO/H_2 reactivity per gram than the reduced-only catalyst. The general trends in Figs. 3 and 4 imply that the reaction sequences of the CO/H_2 reaction over these samples are probably the same. If this is true, the activation energy of these three catalysts should be the same. The activation energies are close for these three catalysts (see also Fig. 5).

Some data on the selectivity of the three

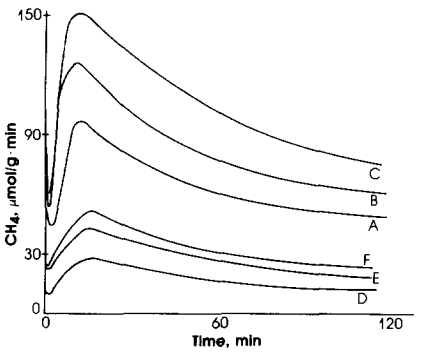

FIG. 4. Rate of CH_4 formation for the CO/H_2 reaction at 558 K over 10% Fe/TiO_2. (A) RDOY, 33% CO/H_2; (B) ROXR, 33% CO/H_2; (C) OXRD, 33% CO/H_2; (D) RDOY, 6.5% CO/H_2; (E) ROXR, 6.5% CO/H_2; (F) OXRD, 6.5% CO/H_2.

catalysts for the CO/H_2 reaction are given in Table 4. The oxidized samples lead to a higher ratio C_1/C_{2+} and to less decrease in this ratio with time on stream.

State of Used Catalysts

Hydrogen titrations. After an unused catalyst is exposed to the CO/H_2 gas stream, it is called a used catalyst. After a certain time of 10% CO/H_2 on stream, the feed into the reactor was switched to H_2 at 558 K. The CH_4 formation during the H_2 titration of the RDOY catalyst is presented in Fig. 6.

TABLE 4

The Ratio of C_1/C_{2+} for the Catalysts Reacted for Various Times in 10% CO/H_2 at 558 K

Reaction time (min)	Sample		
	RDOY	OXRD	ROXR
10	1.52	1.84	1.77
20	1.49	1.88	1.80
30	1.42	1.85	1.74
40	1.36	1.81	1.72
50	1.27	1.78	1.69
120	0.98	1.50	1.36

The CH_4 formation of the OXRD and ROXR catalysts are similar to Fig. 6 except that more CH_4 is formed. Table 5a lists the quantity of CH_4 formed for these three samples during this H_2 titration. The OXRD catalyst forms more CH_4 than the ROXR catalyst and the RDOY catalyst has the least amount of CH_4. Careful study of Fig. 6 has been made and presented in a separate paper (*23*). It was found that there are two active surface species during the CO/H_2 reaction at 558 K. The initial surge in Fig. 6 comes to a maximum value for the CO/H_2 reaction at about 2 min. For longer reaction time, the height of the peak decreases while the total amount of the CH_4 formation increases.

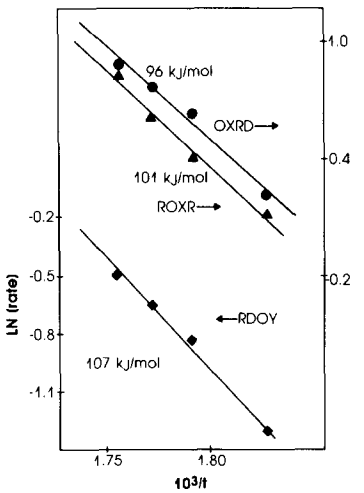

FIG. 5. Arrhenius plot from Fig. 3 for rates at 20 min.

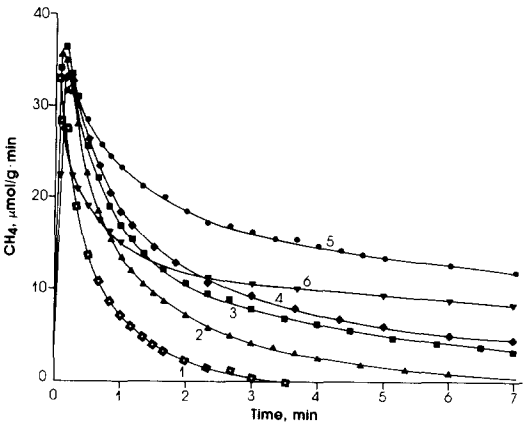

FIG. 6. Methane produced by a switch to hydrogen after various times of 10% CO/H_2 reactions at 558 K, RDOY catalyst. (1) 10 s; (2) 30 s; (3) 60 s; (4) 2 min; (5) 5 min; (6) 10 min.

TABLE 5

CH_4 Formation after the Catalysts are Exposed to 10% CO/H_2 for Various Times and then Switched to H_2 at 558 K

	Reaction time (s)				
	10	30	60	120	300
	(a) CH_4 formation (μmol/g)				
ROXR	53.6	120.0	221.1	413.0	797.2
OXRD	49.7	107.0	194.1	395.2	700.2
RDOY	21.5	46.2	83.3	149.5	383.6
	(b) CH_4 formation (μmol/μmol H adsorbed)				
ROXR[a]	1.06	2.38	4.38	8.19	15.8
	(1.0)[b]	(1.0)	(1.0)	(1.0)	(1.0)
OXRD	0.8	1.71	3.11	6.30	11.2
	(0.75)	(0.71)	(0.71)	(0.76)	(0.71)
RDOY	0.55	1.18	2.15	3.55	9.3
	(0.52)	(0.56)	(0.49)	(0.46)	(0.58)

[a] ROXR is the basis.
[b] The values in parentheses are the relative values to ROXR.

It is instructive to consider the methane produced and listed in Table 5b per unit active site; the same basis as that used to calculate the turnover rate. On this basis it is clear that the oxidized catalysts accumulate more carbon species than the RDOY catalyst, even though their turnover rates for the CO/H_2 reaction are about the same. The relative quantities of CH_4 do not change very much with time, and the following values can be derived: ROXR, 1.0 (basis); OXRD, 0.73; RDOY, 0.51. The calculated results are shown in Table 5b. In what follows we shall see that no bulk carbides are detected until after 6 min, so all this methane has its source in surface carbon-containing species.

Mössbauer results for the catalysts during CO/H_2 reaction. The percentage of carbide formed during the 10% CO/H_2 reaction is plotted against the reaction time in Fig. 7 for the three samples. Owing to space limitations, we present only one set of our Mössbauer spectra in Fig. 8. The bulk-

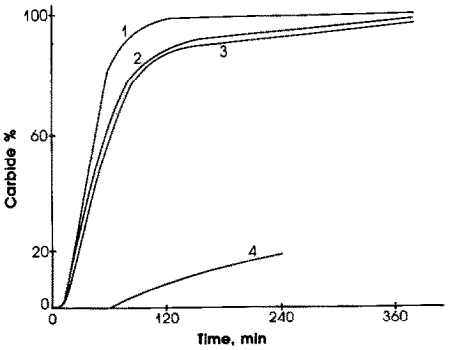

FIG. 7. Carbide formation for iron catalysts during reaction of 10% CO/H_2 at 558 K. Samples: (1) RDOY, (2) OXRD, (3) ROXR, (4) 773 K reduced sample.

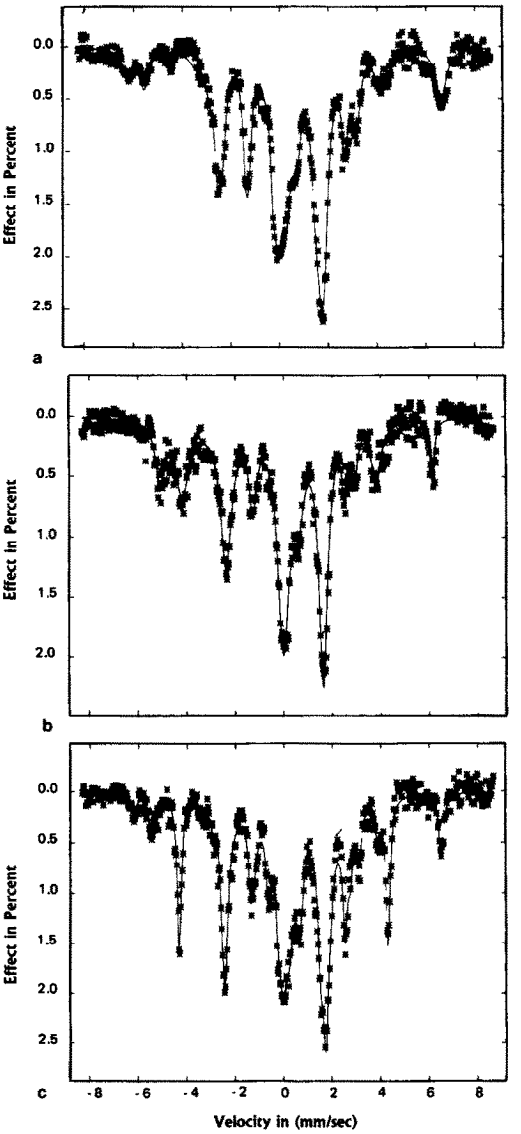

FIG. 8. Mössbauer spectra of Fe/TiO_2 catalysts after exposure to 10% CO/H_2 for 60 min at 558 K. Samples: (a) RDOY, (b) OXRD, (c) ROXR.

phase compositions from Fig. 7 after 60 min. are listed in Table 6. The curve-fitting procedures and constraints were described elsewhere (*3, 4*). Both ε'- and χ-carbides have been found during the carburization process. However, no unknown carbide can be detected. The Mössbauer parameters of ε'- and χ-carbide are shown in Table 7. It can be seen from Fig. 7 that during the first 6 min. of reaction, no bulk-phase carbide can be detected. In other words, the reactivity of the surface carbon with the surface hydrogen is high compared to the rate of diffusion into the bulk phase. In the kinetic study, we found that during the CO/H_2 reaction, CH_4 activity keeps increasing for the initial 10 min. In addition, under the H_2 titration, the height of the CH_4 peaks starts to decrease only when the reaction time is somewhere around 10 min. Both results indicate that the surface species are very active during the first 10 min. of reaction. Our Mössbauer and kinetic results are consistent with each other. The Mössbauer result in this work is different from those of the Fe/SiO_2 and Fe/Al_2O_3 systems under the same reaction conditions. In those systems, some ε'-carbide was found within 10 min (*3*). Figure 7 also shows that after the initial induction period, the carbide formation in these catalysts is rapid for about 60 min. The reaction between surface carbon and Fe is relatively favored over the reaction of surface carbon and hydrogen. Our kinetic results partly support this argument, since we found that the fast carbide formation region corresponds to a declining rate of CH_4 production. This may also be the reason that, during the H_2 titration, the height of the peak decreases when the CO/H_2 reaction time is more than 10 min. Figure 7d presents the carbide formation for the 773 K reduced catalyst and it is completely different from that of the other three catalysts. The slow carburization rate of this high-temperature reduced catalyst has been discussed in a previous paper (*4*). That the SMSI effect can be removed by the high-temperature oxidation is proved again by the Mössbauer results.

TABLE 6

The Bulk-Phase Components Analyzed by Mössbauer Spectroscopy after 60 min of 10% CO/H_2 Reaction

Sample	Fe(0) (%)	Fe^{2+} (%)	$Fe^{8/3+}$ (%)	ε'-Carbide	χ-Carbide
ROXR	22.4	27.1	17.7	11.0	21.8
OXRD	18.0	27.9	19.8	10.0	24.3
RDOY	9.6	28.2	14.2	9.6	38.3

TABLE 7

Mössbauer Parameters of Carbides at T = 298 K

Carbide	Fe site	IS (mm/s)	HF (kOe)
χ-Fe_5C_2	(I)	0.10	190.0
	(II)	0.15	215.0
	(III)	0.19	116.0
ε'-$Fe_{2.2}C$		0.05	174.0

Decarburization after CO/H_2. After 375 min of 10% CO/H_2 on stream, the feed into the system was switched to H_2 to attempt to identify the surface species and to decarburize the bulk-phase carbide. The surface species identification for the RDOY catalyst has been discussed (*23*). Figure 9 presents the Mössbauer spectra of these three catalysts after decarburization for 7 h. It can be seen that there is a great difference among these catalysts. After 7 h decarburization in H_2, the RDOY catalyst contains Fe(0) and Fe(+2) only. However, some carbide is found in the bulk phase of the ROXR and OXRD catalysts. In order to study this matter further, a similar experiment has been carried out by mass spectrometry. After 6 h of 10% CO/H_2 reaction at 558 K, we switched the feed stream to H_2 for 7 h at this temperature then quickly increased the temperature to 723 K (16 K/min) in He followed by switching back to H_2 at this temperature. The results are presented in Figs. 10a and b. In Fig. 10b, we found that the RDOY catalyst contains no

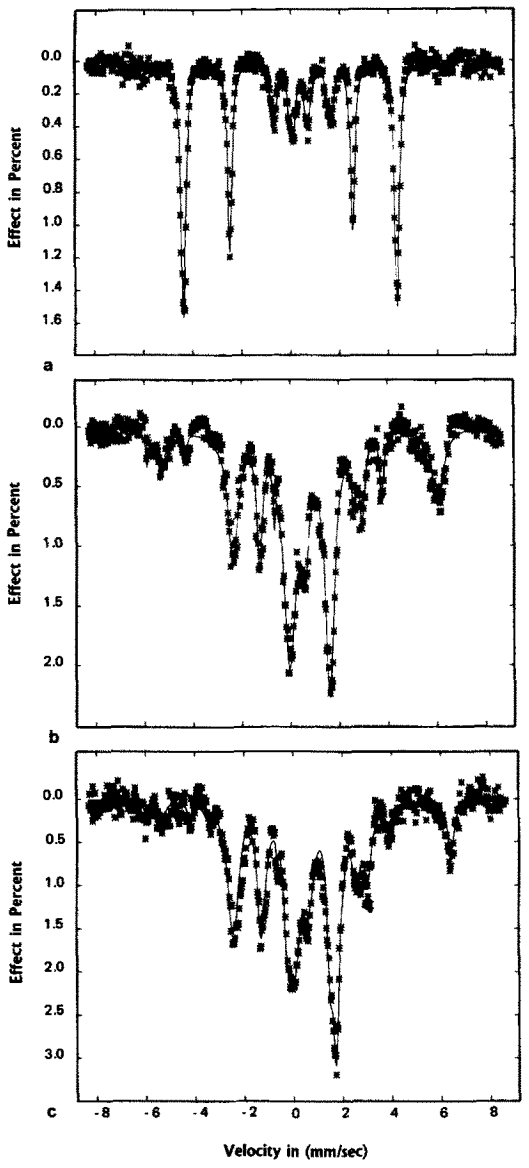

FIG. 9. Mössbauer spectra of 10% Fe/TiO_2 after treating in 10% CO/H_2 for 375 min switch to hydrogen for 7 h at 558 K. Samples: (a) RDOY, (b) OXRD, (c) ROXR.

carbide at all; the others still show lots of carbon in the bulk. This result is consistent with the Mössbauer result. Therefore, we conclude that the decarburization rate for the RDOY catalyst is faster than those of the preoxidized catalysts. A careful study of Fig. 10a provides us with the same conclusion, since after 40 min of H_2 on stream, the rate of CH_4 formation of the RDOY catalyst is higher than the others. In other words, during the H_2 titration process, the bulk-phase carbon has been removed. The slow carburization and decarburization experiments by Mössbauer spectroscopy and mass spectrometry do not imply that the bulk-phase carbide of OXRD and ROXR catalysts cannot be fully obtained or removed. It only implies that the reaction rate of carbon and bulk-phase iron of these preoxidized catalysts are relatively slow when compared with the RDOY catalysts.

In a previous work (*2*), we used the H_2 titration and Mössbauer results to distinguish between the bulk-phase carbide and surface graphite in the Fe/Al_2O_3 system. The decarburization rate for the Fe/Al_2O_3 system has been qualitatively calculated. We were able to do this because of the fast decarburization rate. In the present work, owing to the slow reaction kinetics, there is

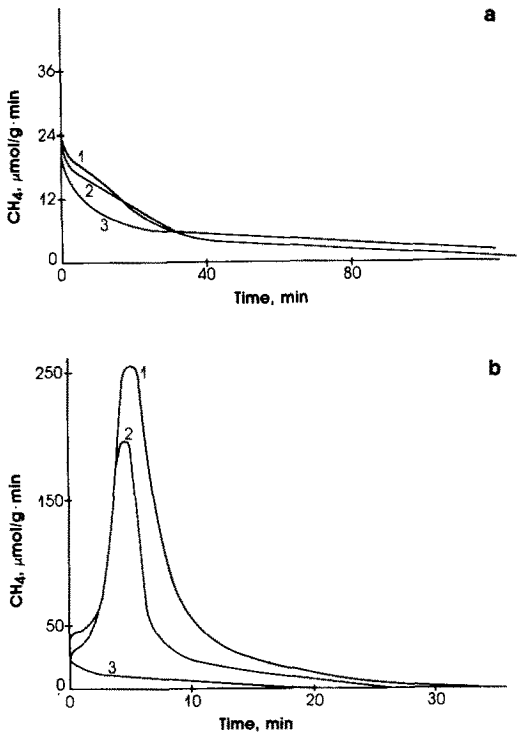

FIG. 10. (a) Methane produced by a switch to hydrogen after 6 h reaction in 10% CO/H_2 at 558 K. Samples: (1) OXRD, (2) ROXR, (3) RDOY. (b) Methane produced by a switch to hydrogen at 723 K of samples of (a). Samples: (1) ROXR, (2) OXRD, (3) RDOY.

no way that we can distinguish the bulk-phase carbide and surface graphite. This makes it difficult to explain the slow decarburization of OXRD and ROXR catalysts. In other words, whether the slow decarburization of these two catalysts is caused by the existence of huge amounts of surface inactive graphite or by the slow bulk-phase kinetics cannot be determined at this moment.

DISCUSSION

The results of this study can be summarized as follows.

1. The crystallite sizes for the ROXR and the OXRD catalysts are slightly lower than those of the RDOY catalyst. The HTRD (SMSI) sample crystallites are almost twice the diameter of those of the other three catalysts (Table 1). Also, some suppression of H_2 chemisorption is observed for this material.

2. The ROXR catalyst, made from HTRD catalyst, shows activity and carburization behavior such that the SMSI effect has been effectively cancelled (Figs. 3 and 7).

3. The catalysts, ROXR, OXRD, and RDOY, show about the same turnover rate at 558 K (100 h^{-1}) and exhibit also about the same bulk composition (Table 2). Their activation energies for the CO/H_2 reaction are similar (100 kJ/ml) (Fig. 5).

4. The selectivities, C_1/C_{2+}, for the two samples pretreated in oxygen are considerably higher than that of the RDOY catalyst (Table 4). However, the amounts of active carbon containing intermediates (detected after 6 min of reaction) are in the ratio ROXR, 1.0; OXRD, 0.73; RDOY, 0.51 (Table 5b). Ordinarily, a higher H/C ratio on the surface leads to a higher C_1/C_{2+} production.

5. The rate of carburization of the two preoxidized samples is considerably lower than that of the RDOY catalyst (Fig. 7). Also, the extent of decarburization after 7 h in H_2 at 558 K is drastically less for the sample pretreated with oxygen than for the RDOY catalyst (Fig. 10b).

To explain the difference in the behavior of the three LTR catalysts we favor the idea that some oxygen is retained in those catalysts treated with oxygen. Since the bulk compositions are similar, and little surface oxygen could not survive during the CO/H_2 reaction, we are led to the postulation of the existence of subsurface oxygen. Geometric surface effects do not seem probable. The presence of the subsurface oxygen must lead to electronic effects that, by some kind of compensation, cause more accumulation of carbon-containing intermediate and higher C_1/C_{2+} selectivity while the turnover rate and activation energy are little changed.

The most dramatic effects of the oxygen treatments are those on the rates of bulk carburization and decarburization. We have shown (*3*) that the surface composition of Fe/Al_2O_3 seems to control the rate of carburization. Thus, it is logical that subsurface oxygen could influence the basis which seems to exist between the surface and the bulk for carbon transfer. The rate of diffusion of C in α-Fe is very high (*3*).

Effects of pretreatments have been seen previously on Group VIII metals. Amariglio *et al.* (*24*) reported that preoxidation of a Rh ribbon increased its activity for ethylene hydrogenation. Taylor *et al.* (*25*) found that preoxidation enhanced the NO reduction activity for Pt and Pd supported on Al_2O_3 but not for Ru/Al_2O_3. Hecker and Bell (*26*) found that preoxidation enhanced the NO reduction 50% for the Rh/SiO_2 system even at a steady state. Dwyer and Somorjai (*27*) found that the oxidized iron catalyst has 10 times the reactivity of the reduced-only catalyst for the CO/H_2 reaction. They suggested this is because the Fe(0) sites created by the reduction of the preoxidized catalyst are more active than those of the reduced-only catalyst. However, those authors noted that the effect of the pretreatment is not a simple function of the catalyst dispersion.

It has been suggested (*4, 7; 8*) that the SMSI for Fe/TiO_2 is caused by migration of

TiO_x onto the surface of the large (250–400 Å) iron particles involved. The TiO_x on iron has a certain geometric effect, since it can alter the distribution of ensembles of iron atoms. However, an electronic effect is also rendered more probable because of the enlarged contact between the iron and TiO_x (*4*). The effective mean size of the iron particles has been increased (Table 1), and the iron crystallite may change their shapes (*17, 18*). After oxidation, Table 3 shows that the iron is all returned to the 3+ state (precursor of the ROXR catalyst). Upon renewed reduction at 558 K the original particle size, chemisorption, and activity are recovered (ROXR $\simeq$ RDOY). However, to explain the differences in selectivity and carburization (ROXR $\neq$ RDOY), we propose that some of the oxygen remains tenaciously held just below the surface of the reduced iron crystallites.

The presence of subsurface oxygen is supported by recent studies. Vasilevich *et al.* (*28*) and Benninghoven *et al.* (*29*) found subsurface oxygen during the course of iron oxidation. Subsurface oxygen was also found in Pd, Ru, Pt, and Ir systems during the course of oxidation (*30–33*). In addition, such subsurface oxygen is resistant to reduction at temperatures below about 600 K. The pressure of this subsurface oxygen would modify the electronic properties of Fe on the surface. Benziger and Madix (*34*) studied the effect of an oxygen adlayer on CO and H_2 adsorption over Fe(100) and found that both CO and H_2 adsorption and dissociation are blocked by the existence of the oxygen adlayer. Their study also showed that the CO blocking is greater than the H_2 blocking. In other words, the iron surface with adlayer oxygen will have higher H/C ratio than the Fe surface without an oxygen adlayer.

These results cannot be carried over completely to our studies at 558 K, where we expect subsurface oxygen and not adsorbed oxygen. However, it was reasonable to expect this oxygen, just below the top iron atoms, to affect the behavior of the catalyst, even if it is not possible to rationalize the directions of all the changes observed. A definitive answer to whether the proposed explanation of our results is true must await experiments which would physically detect (or not) the subsurface oxygen.

ACKNOWLEDGMENT

The support of the National Science Foundation (Grant ENG CPE-81-20499) is gratefully acknowledged.

REFERENCES

1. Bianchi, D., Borcar, S., Teule-Gray, F., and Bennett, C. O., *J. Catal.* **82,** 442 (1983).
2. Bianchi, D., Tau, L. M., Borcar, S., and Bennett, C. O., *J. Catal.* **84,** 358 (1983).
3. Tau, L. M., Borcar, S., Bianchi, D., and Bennett, C. O., *J. Catal.* **87,** 36 (1984).
4. Tau, L. M., and Bennett, C. O., *J. Catal.* **89,** 285 (1984).
5. Tauster, S. J., Fung, S. C., and Garten, R. L., *J. Amer. Chem. Soc.* **100,** 170 (1978); Tauster, S. J., Baker, R. T. K., and Horsley, J. A., *Science (Washington, D.C.)* **211,** 1211 (1981).
6. Takatani, S., and Chung, Y., *J. Catal.* **90,** 75 (1984).
7. Ko, C. S., and Gorte, R. J., *J. Catal.* **90,** 59 (1984).
8. Sadeghi, H. R., and Henrich, V. E., *J. Catal.* **87,** 279 (1984).
9. Meriaudeau, P., Ellestand, O. H., Dufaux, M., and Naccache, C., *J. Catal.* **75,** 243 (1982).
10. Santos, J., and Dumesic, J. A., *Stud. Surf. Sci. Catal.* **11,** 43 (1982).
11. Santos, J., Phillips, J., and Dumesic, J. A., *J. Catal.* **81,** 147 (1983).
12. Freel, J., *J. Catal.* **25,** 139 (1972).
13. Sashital, S. R., Cohen, J. B., Burwell, R. L., Jr., and Butt, J. B., *J. Catal.* **50,** 479 (1977).
14. Amelse, J. A., Schwartz, L. H., and Butt, J. B., *J. Catal.* **72,** 95 (1981).
15. Dalla Betta, R. A., *J. Catal.* **34,** 57 (1974).
16. Jiang, X. Z., Hayden, T. F., and Dumesic, J. A., *J. Catal.* **168,** 83 (1983).
17. Baker, R. T. K., Prestridge, E. B., and Garten, R. L., *J. Catal.* **56,** 390 (1979).
18. Baker, R. T. K., Prestridge, E. B., and Garten, R. L., *J. Catal.* **59,** 293 (1979).
19. Resasco, D. E., and Haller, G. L., *J. Catal.* **82,** 279 (1983).
20. Bichowsky, M. R., and Rossini, F. D., "Thermochemistry of the Chemical Substance." Reinhold, New York, 1936.

21. Aharoni, A., Frei, E. H., and Scheiber, M., *J. Phys. Chem. Solids* **23,** 545 (1962).
22. Boudart, M., Delbouille, A., Dumesic, J. A., Khammouma, S., and Topsøe, H., *J. Catal.* **37,** 486 (1975).
23. Tau, L. M., and Bennett, C. O., *J. Catal.* **89,** 327 (1984).
24. Amariglio, A., Lakhdar, M., and Amariglio, H., *in* "Proceedings, 7th International Congress on Catalysis, Tokyo, 1980," p. 669. Elsevier, New York, 1981.
25. Taylor, K. C., Sinkevitch, R. M., and Kliminisch, R. L., *J. Catal.* **35,** 34 (1974).
26. Hecker, W. C., and Bell, A. T., *J. Catal.* **75,** 251 (1982).
27. Dwyer, D. J., and Somorjai, G. A., *J. Catal.* **52,** 291 (1978).
28. Vasilevich, A. A., Chesnokova, R. V., Minaev, D. M., and Kuznetsov, L. D., *Kinet. Katal.* **29,** 984 (1979).
29. Benninghoven, A., Gauschow, O., and Wiedmann, L., *Ned. Tijdschr. Vacuumtech.* **16,** 22 (1978).
30. Thiel, P. A., Yates, Y. T., Jr., and Weinberg, W. H., *Surf. Sci.* **82,** 22, 45; **90,** 121 (1979).
31. Conrad, H., Ertl, G., Kuppers, J., and Latta, E. E., *Surf. Sci.* **65,** 245 (1977).
32. Klein, K., and Shih, A., *Surf. Sci.* **15,** 443 (1969).
33. Alont, M., Fusy, J., and Cassuto, A., *Surf. Sci.* **72,** 467 (1978).
34. Benziger, J., and Madix, R. J., *Surf. Sci.* **94,** 119 (1980).
35. Bardi, J., Somorjai, G. A., and Ross, P. N., *J. Catal.* **85,** 272 (1984).
36. Belton, D. N., Sun, Y. M., and White, J. M., *J. Phys. Chem.* **88,** 536 (1984).